Microstructure and properties of Cu-rich 123. Part I: Copper at the grain boundaries

J. P. Zhang, D. J. Li, and L. D. Marks
Science and Technology Center for Superconductivity, Department of Materials Science and Engineering, Northwestern University, Evanston, Illinois 60208

C. H. Lin and J. A. Eades
Science and Technology Center for Superconductivity, Materials Research Laboratory, University of Illinois at Champaign–Urbana, 104 South Goodwin, Urbana, Illinois 61801

A. Sodonis, W. Wolbach, J. M. Chabala, and R. Levi-Setti
Science and Technology Center for Superconductivity, The Enrico Fermi Institute and Department of Physics, The University of Chicago, Chicago, Illinois 60637

(Received 2 August 1991; accepted 8 November 1991)

A range of copper-rich bulk $YBa_2Cu_{3+x}O_{7+y}$ superconductors have been prepared by mixing excess copper oxide in the initial material and characterized for their magnetic properties and microstructure. The microstructure of the materials exhibits a high density of planar defects at the grain boundaries and a grain boundary amorphous phase. There is a small increase in the magnetic J_c at 4.5 K but a decrease compared to a conventional material at 77 K, and there is no correlation of the magnetic J_c with the twin boundary density. The change in J_c can be understood if the grain boundary pinning is strong at 4.5 K but weak at 77 K. Data obtained using a very wide range of different microstructure characterization techniques clearly indicate the dangers of relying on only one technique to obtain a full picture of the material.

I. INTRODUCTION

One of the more important issues in the new high temperature superconductors, both technologically and scientifically, is flux pinning; to be a useful material, flux pinning in some form is required for high critical currents. Very early it became apparent that thin films could carry high currents[1–3] and, presumably, contained adequate flux pinning sites. Although there has been recent progress with bulk superconductors, notably melt textured materials,[4–6] bulk materials have yet to achieve critical currents as high as those in thin films. What in the thin films is responsible for the high current carrying properties? For instance, is it planar defects,[7] twin boundaries,[8,9] point defects,[10–13] or is it surface pinning?[14–16]

There have recently been two sets of experiments that have suggested that planar defects may lead to higher critical currents, namely magnetic measurements of decomposed $YBa_2Cu_4O_8$[17] and of shock treated $YBa_2Cu_3O_7$.[18] In this paper we report the results of a controlled comparison of copper-rich bulk $YBa_2Cu_{3+x}O_{7+y}$ superconductors prepared with excess copper in the initial material. Although there is a small enhancement of the flux trapping at 4 K, the materials are in fact inferior to conventional $YBa_2Cu_3O_7$ at 77 K. There is definitely no correlation of the magnetic J_c with the twin boundary density. In a later paper,[19] we will present results using copper oxide dissolved in nitric acid and added to 123 powder where precipitates are formed throughout the material and flux pinning does occur. These results indicate that the reaction kinetics of the added copper is critical to determining the magnetic properties of the resulting superconductor.

II. SPECIMEN PREPARATION

Samples were prepared by sintering a mixture of Y_2O_3, $BaCO_3$, and CuO powders in stoichiometric proportions to obtain $YBa_2Cu_{3+x}O_{7+y}$ nominal compositions with $x = 0$, 0.2, 0.5, and 1.0. Sintering was carried out at 938 °C for 20 h in air and then quenched into liquid nitrogen. (From previous work,[20] it appeared that to retain the additional copper in the material prepared by this route it is necessary to quench into liquid nitrogen.) Following this quench, two different annealing conditions were tested: (a) Annealing with a slow temperature rise from room temperature to 900 °C (18 h) in an oxygen atmosphere, continued to 20 h at 900 °C followed by a slow cool (18 h) to room temperature. This produced a conventional $YBa_2Cu_3O_7$ superconductor which was used as a control. (b) Rapid annealing by placing the samples into a preheated furnace at 900 °C, continuing at this temperature for 30 h also in oxygen, followed by the same slow cool as in (a). The second annealing treatment was tested for nominal compositions $YBa_2Cu_{3+x}O_{7+y}$ with $x = 0$, 0.2, 0.5, and 1.0.

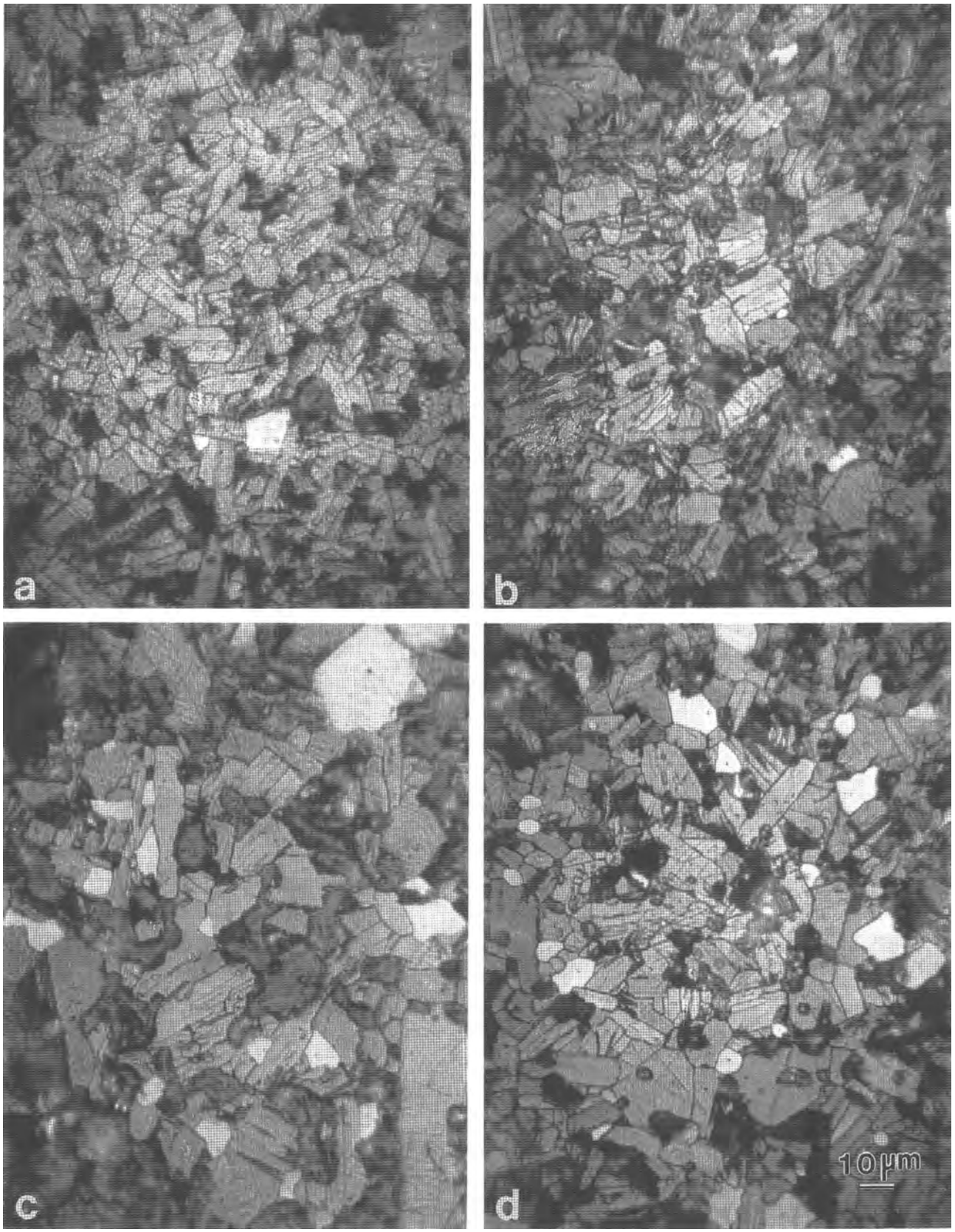

FIG. 1. Optical metallographs of the rapidly annealed samples: (a) 1:2:3; (b) 1:2:3.2; (c) 1:2:3.5, and (d) 1:2:4.

III. MAGNETIC AND MICROSTRUCTURE CHARACTERIZATION

To avoid errors in the interpretation, we should stress that it is critical to exhaustively characterize the samples. The magnetic measurements were performed using a Quantum Design SQUID (Superconducting Quantum Interference Device), and measurements for the range of compositions and annealing conditions were performed at both 4.5 K and 77 K. The lower resolution microstructure was investigated using samples that were mechanically polished with oil-diluted diamond paste and then etched by a 3% bromine solution in ethyl alcohol and then examined by optical microscopy, Scanning Electron Microscopy (SEM), and Secondary Ion Mass Spectroscopy (SIMS) imaging analysis with a high resolution Scanning Ion Microprobe.[21] The higher resolution microstructure was examined by High Resolution Electron Microscopy (HREM) of the crushed powder and Scanning Transmission Electron Microscopy (STEM) and HREM of ion beam thinned samples.

IV. RESULTS

For convenience, we will break down the results into a number of sections on the large-scale microstructure, the atomic-scale microstructure, and the magnetic properties.

A. Large-scale microstructure

Results from optical microscopy, SEM, and SIM indicated that the material consisted of large Cu_2O/CuO grains, 123 material, and voids. (We estimate that the density of the material was 70–90% of the theoretical density.) Typical optical micrographs are shown in Fig. 1, and the SIMS micrograph in Fig. 2 confirms the presence of large Cu-rich grains. By comparison of the Cu^- and O^- secondary ion intensities with those emitted by the minerals cuprite (CuO) and tenorite (Cu_2O), it was deduced that these grains consisted of ~90% Cu_2O and ~10% CuO. Analysis of the optical micrographs gave a log-normal grain size distribution (see Fig. 3) with the results for the different samples summarized in Table I. The O^- SIMS signal intensity emerging from the sample crystallites (other than the Cu_2O/CuO grains) was consistent with that obtained from the control 123 superconductor indicating the orthorhombic phase, and this was confirmed by the observation of twins in the material by electron microscopy; see Fig. 4.

An interesting feature of the SIM/SIMS images is that they exhibit crystallographic contrast from the twin structures due to primary ion channelling effects[22]; a typical image obtained with the mass unresolved signal is shown in Fig. 5(a), and the corresponding analytical image from the resputtered Ga^+ signal (the SIM uses a 40 kV Ga^+ probe) is shown in Fig. 5(b). In Fig. 5(a), the detector is at a shallow angle to the sample surface so a small amount of surface relief from differential etching also provides some topographic contrast. This makes it feasible to readily identify twins even at low magnifications and has enabled a statistical survey to be obtained of the relative frequency of the occurrence

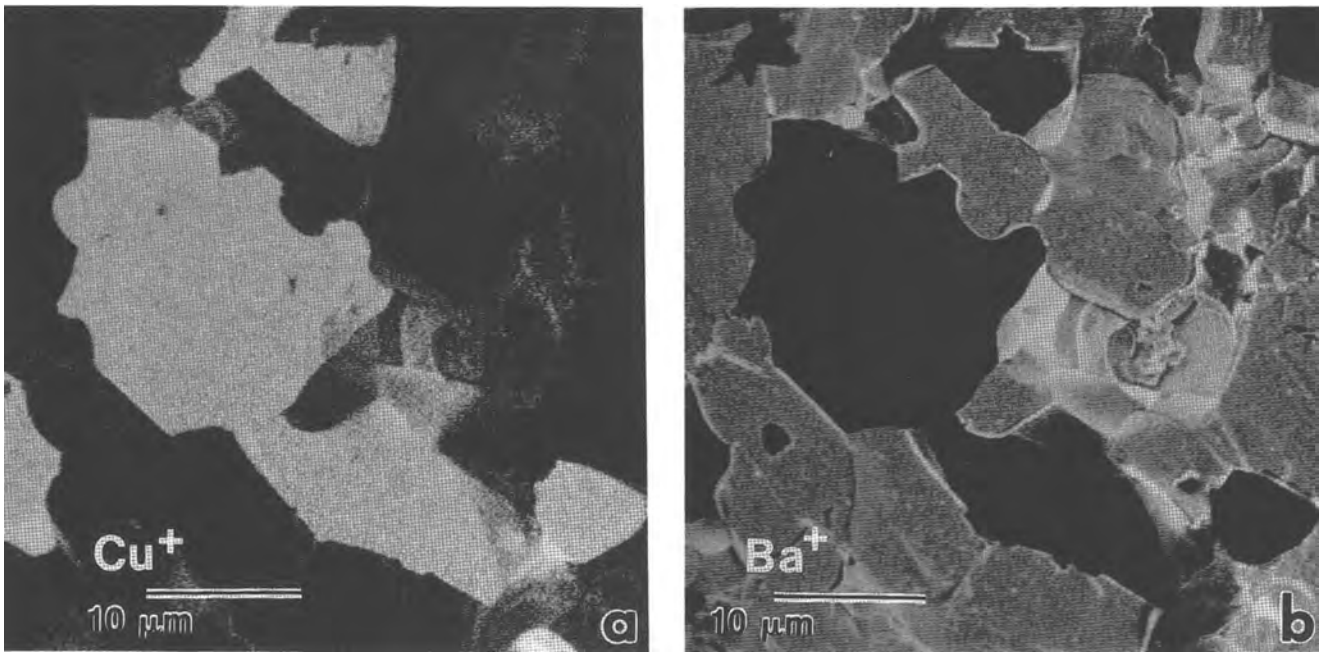

FIG. 2. SIMS images of the $x = 1$ sample obtained with the University of Chicago scanning ion microprobe (UC SIM). Figure (a) is a Cu^+ map, showing the existence of large Cu-rich grains (mostly Cu_2O). Figure (b) is a map of Ba^+, originating from the 123 crystallites. Local intensity enhancements result from the cos θ^{-1} dependence of the emission yields (edge effects) and indicate the presence of cavities and crevices.

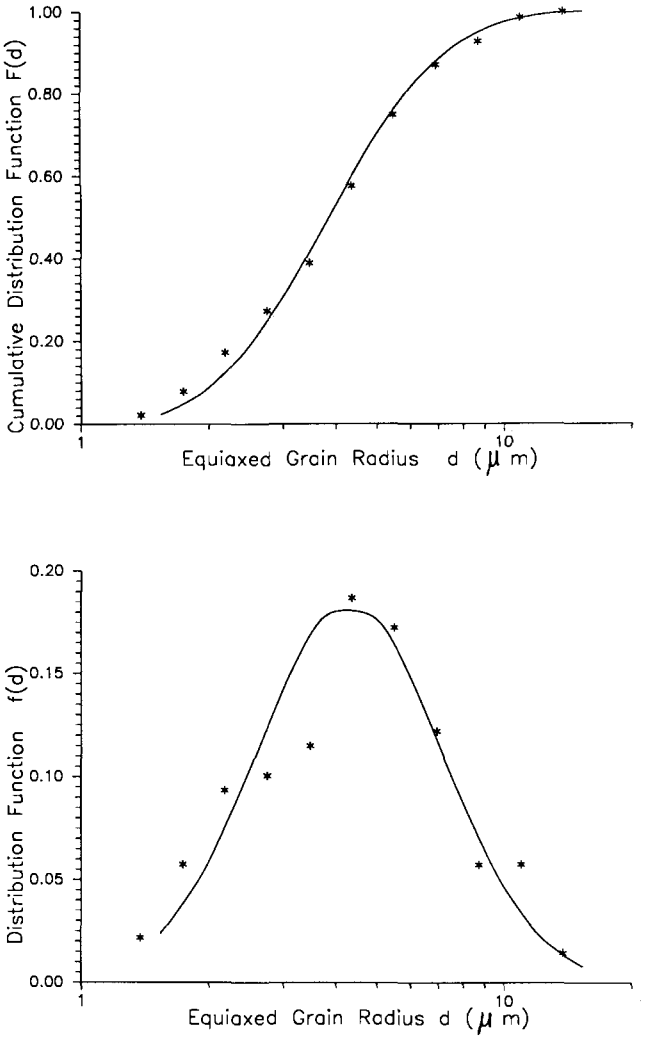

FIG. 3. A typical log-normal cross-sectional size distribution for the 123 control sample. With the assumption that the Bean model magnetization is the sum of 2-D plates, the effective radius can be taken as the mean.

of twins among the sample grains. The results of this survey are contained in Table I.

B. Atomic-scale microstructure

Two techniques of sample preparation were used for the electron microscopy, namely crushing the powder and ion beam thinning. The two give different views of the material, and either one alone might be misleading.

The crushed samples showed a high density of planar defects[23–25] near the surface; see, for instance, Fig. 6(a) which shows a sample prior to the annealing. Similar to our earlier work, the planar defects ordered somewhat with annealing. We should mention that the planar defects are primarily straight, but do step along the (001) direction [see Fig. 6(b)]. Steps of this sort correspond to dislocations with a c-axis Burgers vector. We should also mention that the surfaces of the materials were amorphous; this is an important point whose relevance will become more apparent below and was not a consequence of electron beam or water damage.[26]

The ion beam thinned samples, see Fig. 7, showed that the majority of the material was perfect 123, with the defects restricted to the region immediately at the grain boundaries. A typical width of this region was 100 nm. They also showed the presence of a copper-rich (from EDX in an HB5 STEM) amorphous region at the boundary.

The two sets of results can be connected if we recognize that on crushing, the material will tend to break at the amorphous grain boundary phase. This explains the observation of many defects in the crushed samples and the presence of an amorphous surface phase; the crushed samples are selectively showing the grain boundary phase. This also allows us to rule out the possibility of ion-beam damage during sample preparation as a source of the grain boundary phase or the defects.

C. Magnetic properties

The primary magnetic property that we will focus on is the magnetic hysteresis. From the standard Bean Model,[27] this can be used to calculate the J_c for the individual grains. We note that more sophisticated models[28,29] lead only to different constants in the model so will lead only to some constant scaling of the results.

Table II summarizes the J_c values calculated in this fashion, taken at temperatures of 4.5 K and 77 K. Whereas there is a small increase in the apparent J_c at 4.5 K, particularly for the material of nominal composi-

TABLE I. Twinning and Cu_2O/CuO crystal distributions. The mean radius was based on a larger number of particles than the mean cross-sectional area measurements.

Sample	1:2:3	1:2:3.5	1:2:4	1:2:3 (control)
Crystals showing twins (%)	8.8	8.8	8	2.2
Twins/μ^2	0.1	0.06	0.1	0.06
Cross section (μ^2)	34.5	58.4	30.7	16.0
CuO crystal area (%)	0.0	1.2	7.1	0.0
CuO crystals/μ^2	...	0.02	0.06	...
Cross section CuO (μ^2)	...	23.6	45.9	...
Mean radius (μ)	4.8	4.9	4.5	3.0

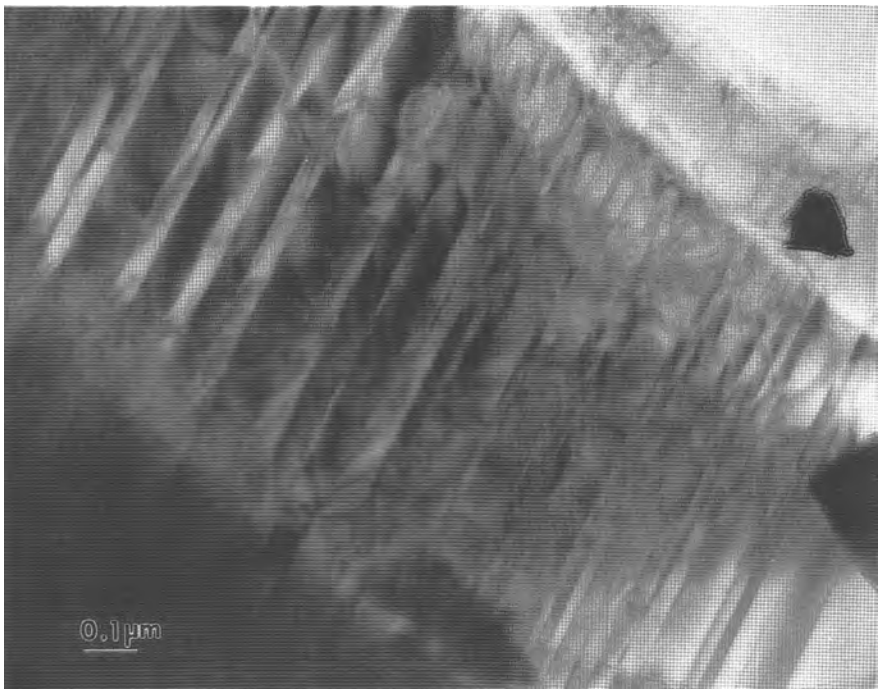

FIG. 4. Conventional transmission electron micrograph showing the characteristic twin structure of orthorhombic 123.

tion 123.5, there is a drop at 77 K which goes in exactly the opposite direction.

V. DISCUSSION

The microstructure that we have produced here is bulk $YBa_2Cu_3O_{7-y}$ with a high density of planar defects at the grain boundaries. If these planar defects are strong flux pinning sites, one would expect an enhancement of the J_c in these materials. Whereas there is a small enhancement at 4 K, at 77 K the J_c is slightly worse, and the conventionally produced material has, in fact, very good properties. There is a very simple model that we will propose to explain this, namely that the grain

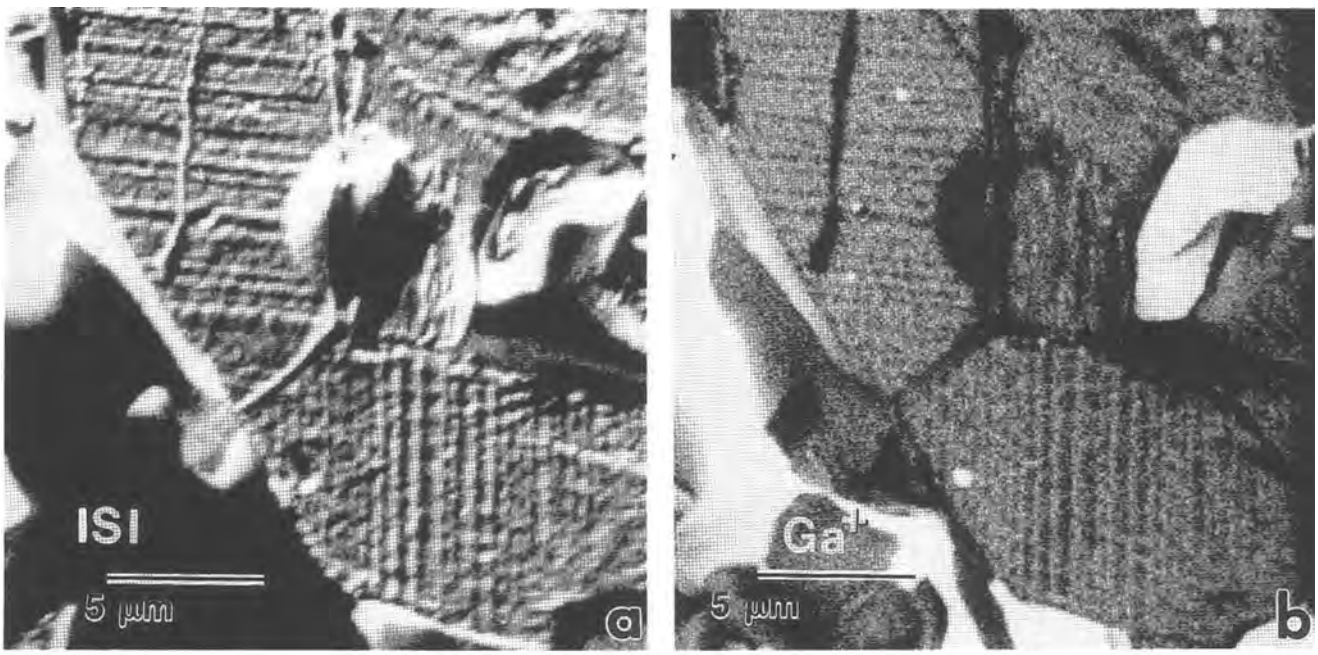

FIG. 5. Twin structures in crystallites of the $x = 1$ sample, detected in the UC SIM. In (a), an image with the mass unresolved secondary ions and in (b) the resputtered Ga^+ signal.

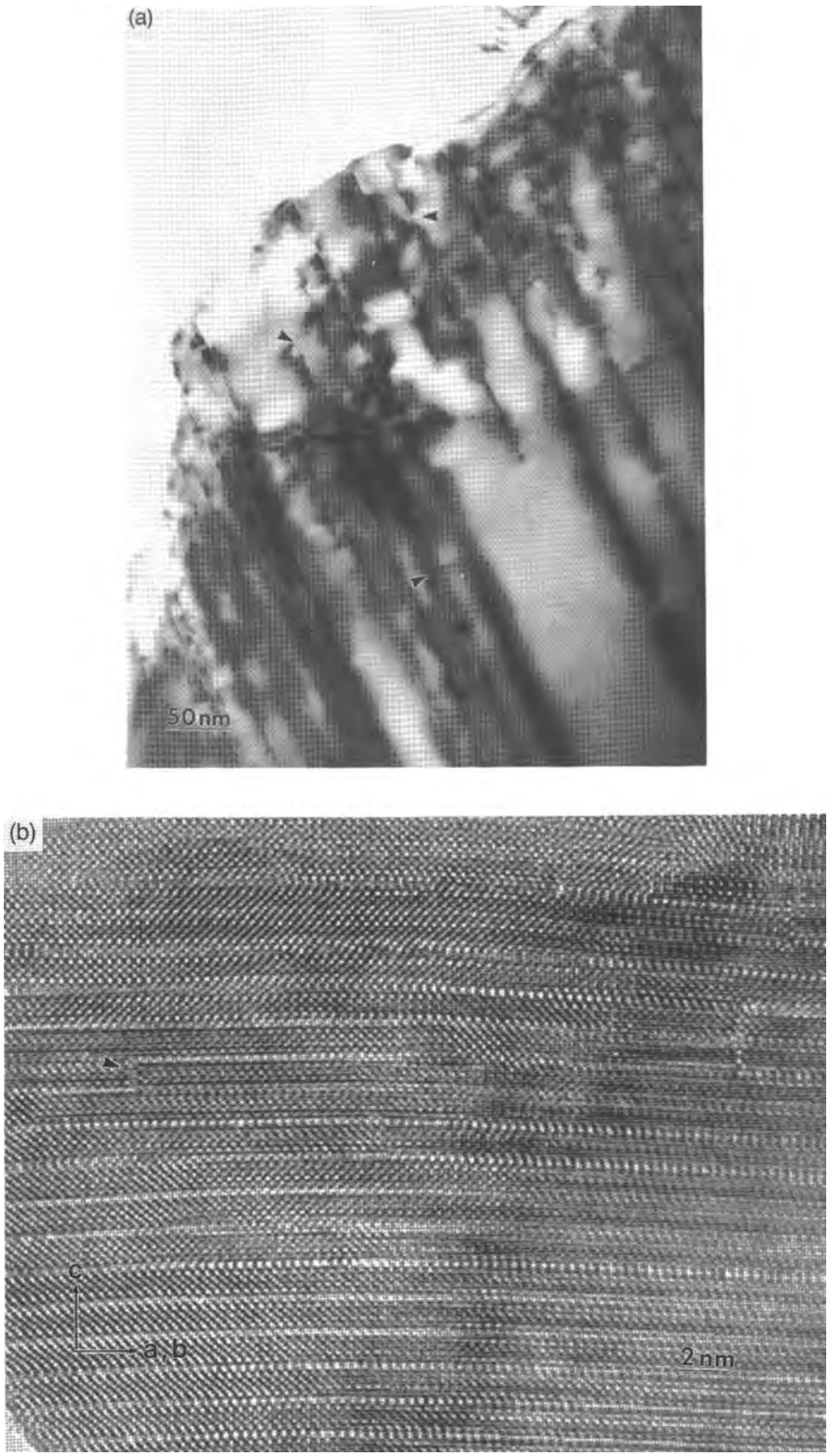

FIG. 6. (a) Transmission electron microscope images showing the planar defects (strong dark lines) near the crystal edge. The black/white contrast (arrowed) at places along the defects is due to the strains associated with the dislocations when the defect plane changes. (b) High resolution image showing more clearly the stepping of the defects, arrowed.

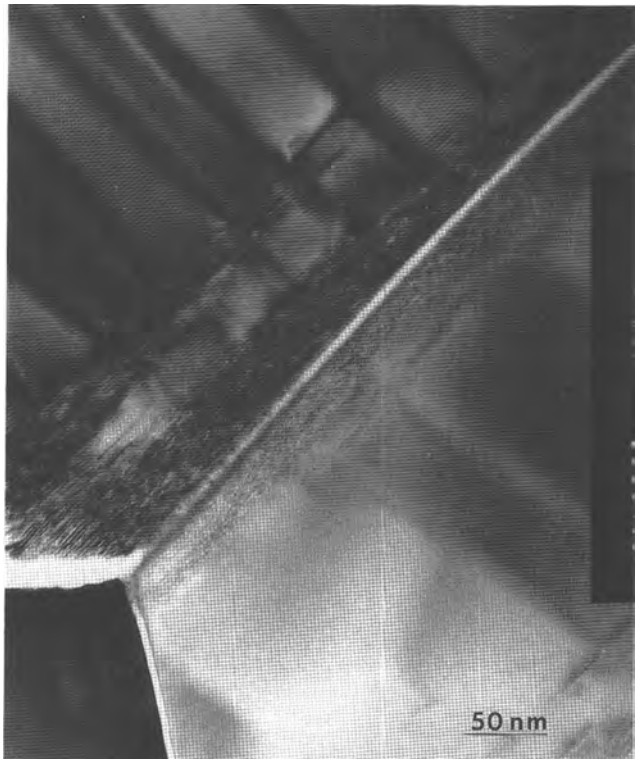

FIG. 7. Transmission electron microscope image showing the copper planar defects localized to the grain boundary region only. At some (not all) of the boundaries, including the ones shown here, there is a copper-rich amorphous phase.

boundary region is a flux pinning superconductor at 4.5 K, but not, or at least a poor pinning superconductor, at 77 K.

Although these results are disappointing in some respects, there are some important points to be made from this work. First, we should mention that the grain size was log-normal. Provided that one works within a Bean or Bean-like model, the relationship between J_c and the grain size is linear so it is appropriate to use a mean grain size. However, if this is not the correct model and the relationship is nonlinear, there exists room for substantial error.

Second, it is apparent that there is a small change in the twin boundary density among the different samples, but no clear correlation with the magnetic results. This is not too surprising; results from single crystals[9] indicate that the flux pinning strength of twin boundaries is comparatively small, so one would not expect it to be a substantial contributor. However, it is still relevant to confirm this fact in a polycrystalline sample.

Third, it is apparent that many different microanalytical techniques are needed to give a full picture of the material. The important point here is that each technique provides only selective information, and alone can be misleading. This is most clearly evident with the crushed samples which appear to be only sampling the grain boundary regions. Since this is the simplest method of making samples for high resolution electron microscopy, one has to question the appropriateness of some of the published data in terms of being representative of the sample as a whole.

Finally, to end on a slightly more optimistic note, we should mention that with a different sample preparation approach the defects can be forced from the grain boundaries into the material as a whole, and this does lead to much better properties.[19] It appears that magnetization truly does measure the matrix of the materials and is sensitive to the matrix flux pinning rather than the intergranular effects which are better probed by transport measurements. For completeness, it should be mentioned that the transport J_c of these materials was low (~200 A/cm^2 at best), although there were some unusual hysteretic effects in a magnetic field which will be described elsewhere.

TABLE II. Bean model J_c using the mean cross-sectional radius for different compositions, treatments, and field together with the mean cross-sectional data. Note that there is a small increase in J_c at 4 K which is maximum for the nominal composition 1:2:3.5 and a corresponding decrease at 77 K.

		4.5 K, × 10^6 A/cm^2				77 K, × 10^3 A/cm^2			
Composition	Rad (μ)	0.1 T	1 T	3 T	4 T	0.1 T	1 T	3 T	4 T
Rapid anneal									
1:2:3	4.8	10.0	5.4	1.6	1.3	52	1.4	1.0	1.0
1:2:3.2	4.8	10.9	6.4	2.3	1.4	76	1.6	0.8	0.4
1:2:3.5	4.9	15.4	9.4	6.2	3.2	58	0.9	0.6	0.6
1:2:4	4.5	8	4.4	1.3	0.9	42	1	1.3	0.3
Slow anneal (control)									
1:2:3	3.0	10.8	5.7	1.5	0.8	133	3.9	1.0	1.0

ACKNOWLEDGMENTS

This work was supported by the Science and Technology Center for Superconductivity on Grant No. NSF/DMR-8809854.

REFERENCES

1. K. Watanabe, Appl. Phys. Lett. **54**, 575 (1989).
2. X. X. Xi, G. Linker, O. Meyer, E. Nold, B. Obst, F. Ratzel, R. Smithey, B. Strehlan, F. Weschenfelder, and J. Geerk, Z. Phys. B **74**, 13 (1989).
3. G. Koren, A. Gupta, E. A. Giess, A. Segmüller, and R. B. Laibowitz, Appl. Phys. Lett. **54**, 1054 (1989).
4. S. Jin, T. H. Tiefel, R. C. Sherwood, M. E. Davis, R. B. van Dover, G. W. Kammlott, R. A. Fastnacht, and H. D. Keith, Appl. Phys. Lett. **52**, 2074 (1988).
5. K. Salama, V. Selvamanickam, L. Gao, and K. Sun, Appl. Phys. Lett. **54**, 2074 (1988).
6. R. L. Meng, C. Kiinalidis, Y. Y. Sun, L. Gao, Y. K. Tao, P. H. Hor, and C. W. Chu, Nature **345**, 326 (1990).
7. V. Selvamanickam and K. Salama, "Superconductivity Applications and Developments," Winter Annual Meeting of ASME MD **11**, 35 (1988).
8. P. H. Kes, A. Pruymboom, J. van den Berg, and J. A. Mydosh, Cryogenics **29**, 1189 (1989).
9. U. Welp, W. K. Kwok, G. W. Crabtree, K. G. Vandervoort, and J. Z. Liu, Appl. Phys. Lett. **57**, 84 (1990).
10. Y. Matsui, E. Takayama-Muromachi, and K. Kato, Jpn. J. Appl. Phys. **26**, L1183 (1987).
11. B. Roas, B. Hensel, G. Saemann-Ischenko, and L. Schultz, Appl. Phys. Lett. **54**, 1051 (1989).
12. R. B. van Dover, E. M. Gyorgy, L. F. Schneemeyer, J. W. Mitchell, K. V. Rao, R. Puzniak, and J. V. Waszczak, Nature **342**, 55 (1989).
13. Shigemi Kohiki, Shin-ichiro Hatta, Kentaro Setsune, Kiyotaka Wasa, Yasuhiro Higashi, Sei Fukushima, and Yohichi Gohshi, Appl. Phys. Lett. **56**, 298 (1990).
14. D. Shi, M. S. Boley, V. Welp, J. G. Chen, and Y. Liao, Phys. Rev. B **40**, 5255 (1989).
15. M. Murakami, M. Morita, K. Doi, and K. Miyamoto, Jpn. J. Appl. Phys. **28**, 1189 (1989).
16. K. Watanabe, T. Matsushita, N. Kobayashi, H. Kawabe, E. Aoyagi, K. Hiraga, H. Yamane, H. Kurosawa, T. Hirai, and Y. Muto, Appl. Phys. Lett. **56**, 1490 (1990).
17. S. Jin, T. H. Tiefel, S. Nakahara, J. E. Graebner, H. M. O'Bryan, R. A. Fastnacht, and G. W. Kammlott, Appl. Phys. Lett. **56**, 1287 (1990).
18. S. T. Weir and W. J. Nellis, Appl. Phys. Lett. **56**, 2042 (1990).
19. D. J. Li, C. Boldt, J. P. Zhang, V. Dravid, L. D. Marks, A. Sodonis, W. Wolbach, J. M. Chabala, and R. Levi-Setti, *in preparation.*
20. D. J. Li, H. Shibahara, J. P. Zhang, and L. D. Marks, Physica C **156**, 201 (1988).
21. R. Levi-Setti, Y. L. Wang, and G. Crow, Appl. Surf. Sci. **26**, 249 (1986).
22. R. Levi-Setti, T. R. Fox, and K. Lam, Nucl. Instrum. Methods **205**, 299 (1983).
23. L. D. Marks, D. J. Li, H. Shibahara, and J. P. Zhang, J. Electron Microsc. Technique **8**, 297 (1988).
24. H. W. Zandbergen, R. Gronsky, K. Wang, and G. Thomas, Nature **331**, 596 (1988).
25. H. Shibahara, L. D. Marks, S-J. Hwu, and K. R. Poeppelmeier, J. Solid State Chem. **79**, 194 (1989).
26. J. P. Zhang, D. J. Li, and L. D. Marks, in *High-Temperature Superconductors,* edited by M. B. Brodsky, R. C. Dynes, K. Kitazawa, and H. L. Tuller (Mater. Res. Soc. Symp. Proc. **99**, Pittsburgh, PA, 1988), p. 965.
27. C. P. Bean, Phys. Rev. Lett. **8**, 250 (1962).
28. C. P. Bean, Rev. Mod. Phys. **36**, 31 (1964).
29. P. W. Anderson and Y. B. Kim, Rev. Mod. Phys. **36**, 39 (1964).